Ocean and Coastal Management 178 (2019) 104799

Contents lists available at ScienceDirect

Ocean and Coastal Management

journal homepage: www.elsevier.com/locate/ocecoaman

Comparison of Coastal Vulnerability Index applications for Barcelona Province

Aysun Koroglu[a,b,*], Roshanka Ranasinghe[a,c,d], José A. Jiménez[e], Ali Dastgheib[a]

[a] Department of Water Science and Engineering, IHE Delft Institute for Water Education, P.O. Box 3015, 2601, DA, Delft, the Netherlands
[b] Department of Civil Engineering, Istanbul Technical University, Ayazaga Campus, P.O. Box 34469, Maslak, Istanbul, Turkey
[c] Harbour, Coastal and Offshore Engineering, Deltares, P.O. Box 177, 2600, MH, Delft, the Netherlands
[d] Department of Water Engineering and Management, University of Twente, P.O. Box 217, 7500, AE, Enschede, the Netherlands
[e] Laboratori D'Enginyeria Marítima, Universitat Politècnica de Catalunya-BarcelonaTech, C/ Jordi Girona, 1-3, Campus Nord Ed D1, 08034, Barcelona, Spain

ARTICLE INFO

Keywords:
Coastal vulnerability index
Coastal zone
Vulnerability
Barcelona
Python
GIS

ABSTRACT

The Coastal Vulnerability Index (CVI) is one of the simplest and commonly used methods to assess coastal vulnerability to sea-level rise (SLR) driven erosion and/or inundation. In this way, it is a common tool contributing to the decision-making process in long-term coastal planning and management. However, there is not a unique approach to be adopted, and existing ones can supply different information and, thus, promote different decisions. Within this context, the main goal of this paper is to compare and evaluate different methodologies to determine CVI, and to suggest the most appropriate approach that can be generically applied for coastal vulnerability assessment. For doing this, the approaches proposed by Gornitz (1991), Shaw et al. (1998), Thieler and Hammar-Klose (2000), and Lopez et al. (2016) are applied along the 160 km long the Barcelona coastline in the Spanish Mediterranean.

Shaw et al.'s (1998) method appears to be the more realistic approach to assess vulnerability of the Barcelona coast while the overall vulnerability level calculated by the equation proposed by Gornitz (1991) indicate a wide variability, from highly vulnerable to a very low level of vulnerability. This study shows that the ranking tables generated from site-specific databases may not be applicable elsewhere, and indicates that it might be prudent to develop site or region-specific ranking categories to compute the overall CVI in order to provide reliable inputs to local coastal zone management initiatives. Despite the potential bias in the categorization of the overall CVI classes and their expert opinion/judgment approval requirements, CVI tools help decision makers to take the necessary actions to increase the resilience of coastal zones to SLR.

1. Introduction

A significant and growing number of residents in the European Union (EU) live in coastal regions. Nearly 19 percent of the population (around 86 million people) are living within 10 km of the coastal strip (EEA, 2006), and close to 50 percent of the population (around 200 million people) (ESTAT, 2009) are living within 50 km of a European coastline. Due to the anthropogenic effects, the sea level rose by 0.06 m during the nineteenth century and 0.19 m in the twentieth century (Svetlana et al., 2008). Approximately 140.000 km^2 of EU land is 1 m above sea level, and in some countries, low-lying coastal areas are densely inhabited (e.g., Denmark, England, Germany, Italy, and the Netherlands) (EEA, 2010), making coastal ecosystems and people who benefit from coastal services vulnerable to potential sea-level rise (SLR).

Climate models typically focus on the projections of global SLR by 2100, based on varying assumptions, and attempt to explain the increase in greenhouse gas emissions and melting ice sheets in Greenland and the West Arctic, as well as the sea level's response to increasing global surface air and ocean water temperature.

Climate projections, similar to those of the Intergovernmental Panel on Climate Change IPCC, (2001),IPCC et al., 2007, 2014) are increasingly used in decision-making. The most recent projections presented by the Fifth Assessment Report (AR5), consider a scenario of very high emissions and predict a global SLR of 0.52–0.98 m by the end of this century. Representative Concentration Pathway (RCP) scenarios are based on a greenhouse gas concentration trajectory adopted by the IPCC in the AR5. In spite of this, there are other studies predicting larger SLR as Vermeer and Rahmstorf (2009) who used a semi-empirical method linking temperature changes to SLR, and the resulting projected global SLR of 0.75–1.9 m which is significantly higher than the IPCC

* Corresponding author. Department of Water Science and Engineering, IHE Delft Institute for Water Education, P.O. Box 3015, 2601, DA, Delft, the Netherlands.
E-mail address: koroglua@itu.edu.tr (A. Koroglu).

https://doi.org/10.1016/j.ocecoaman.2019.05.001
Received 6 November 2018; Received in revised form 25 April 2019; Accepted 4 May 2019

AR5 projections.

While these projections estimate the likely SLR rates for different climate scenarios, severe impacts on coastal regions, rivers systems, and urban infrastructures has already been observed. The permanent inundation of coastal areas results with shoreline erosion, declining water quality, decreasing fish cultivation, seawater intrusion to freshwater resources, the inundation of wetlands and estuaries, and a declining water quality, are listed as the drastic consequences of SLR due to climate change.

SLR will lead to coastal recession (Bruun, 1962; Ranasinghe et al., 2012; Ranasinghe and Stive, 2009), coastal flooding (e.g. Aucelli et al., 2018; Woodruff et al., 2013; Nicholls et al., 2008), subsidence (e.g. Aucelli et al., 2017) and may decrease the efficacy of existing coastal protection structures (e.g., overtopping of breakwaters, groins, seawalls, and dikes, e.g. Arns et al., 2017). In extreme cases, an existing effective coastal protection structure may be exposed to erosion due to SLR (Ranasinghe, 2016). Climate change is also expected to affect storm wave characteristics and storm surges in the coming decades (Bennett et al., 2016; Hemer et al., 2012; Sterl et al., 2009; Nicholls et al., 2007; IPCC, 2001), due to warming of the oceans and atmosphere. If storm patterns and wave distributions are changed, coastline shapes will tend to adjust to the new condition. It is a process involving greatly accelerated shoreline erosion in many areas that will affect coastal communities and infrastructure (Slott et al., 2006). Ranasinghe (2016) stated that increased storm induced erosion may pose a more damaging coastal impact than a slow, gradual erosion due to SLR. Climate change also affects rivers systems. Ranasinghe et al. (2013) pointed out that the 40 percent of change in annual river flow (IPCC et al., 2013) and/or fluvial sand supply in the estuary/lagoon will further increase (or decrease), due to the additional (reduced) demand of sand by the basin to maintain equilibrium velocities within the estuary/lagoon.

The vulnerability concept is explained in various ways by the experts from different disciplines. Gouldby and Samuels (2005) defined vulnerability using the Source-Path-Receptor-Consequences conceptual model as a characteristic of a system that describes its potential to be harmed. IPCC et al. (2014) states that exposure and vulnerability are influenced by a wide range of social, economic, and cultural factors and processes that have been incompletely considered to date, which make quantitative assessments of their future trends difficult (high confidence). These increasing effects of climate change on the coastal zone has confronted the coastal zone managers and decision makers usually with the limited resources and the question of where to invest. To make this decision rational, vulnerability analysis is necessary along the coast indicating the relative vulnerability of different areas.

Although the first tool-based initiative to evaluate the coastal vulnerability to SLR was developed by Carter (1990), the Sensitivity Index was named a more simplistic approach based on a preliminary coastal hazards database developed by Gornitz and Kanciruk (1989). The methodology of Gornitz and Kanciruk (1989) became one of the simplest, commonly used methods to assess coastal vulnerability to SLR, particularly due to erosion and/or inundation. Their initial aim was to develop a coastal hazards' database to provide a global overview of the relative vulnerabilities of the world's coastlines to inundation and erosion hazards associated with accelerated SLR. To reflect the physical vulnerabilities of coastal regions, an improved version of this database was named the Coastal Vulnerability Index (CVI), using the coastal geomorphology, regional coastal slope, relative sea-level change, mean significant wave height, historical shoreline change rate, and the mean tidal range (Gornitz and Kanciruk, 1989). Additional to these listed physical land and sea variables, Gornitz (1991) and Gornitz et al. (1994) modified the CVI to distinguish the effects of severe storms on coastal vulnerability by adding six more climatological variables, such as the annual tropical storm probability, the annual hurricane probability, a hurricane frequency and intensity index, the mean forward velocity, the annual mean extra-tropical cyclones, and the mean hurricane surge.

The CVI approach proposed by Gornitz (1991) and Gornitz et al. (1994), has been applied and/or adapted by numerous researchers to assess coastal vulnerability around the world coastlines (e.g. Shaw et al., 1998; Thieler and Hammar-Klose, 1999, 2000; Pendleton et al., 2004: Boruff et al., 2005; Doukakis, 2005; Diez et al., 2007; Nageswara Rao et al., 2008; Ozyurt and Ergin, 2010; Abuodha and Woodroffe, 2010; Lopez et al., 2016). CVI results can be used to highlight regions in which factors contribute to shoreline changes and may have the greatest potential to contribute to changes to shoreline retreat (Gutierrez et al., 2009). Despite the robustness of CVI application plans for climate change adaptation, the results require the need for an expert opinion/judgement in the computation of vulnerability indices due to the bias recorded in categorizations. Gibb et al. (1992) explained the deficiency as the tendency to distort the output range and distribution of the final index. On the other hand, expert opinion or judgment has been commonly used to validate the findings of vulnerability assessments, deciding on appropriate climate change adaptation plans, or concerns on the thresholds of climate change events (Brooks and Adger, 2005; Doria et al., 2009; Arnell et al., 2005; Smith et al., 2009). On the other hand, against the reported deficiencies of CVI tools by means of output range distortions, nearly 30 percent % of the studies on coastal vulnerability used this methodology (Cogswell et al., 2018).

There have been also several approaches for vulnerability analysis that requires different types of data within different ranges and formulas. For instance, besides the characterization of physical elements, some vulnerability indexes also integrate the socio-economic variables. These indexes include total population versus the total population affected by floods, population density, the total non-local population, poverty levels, and municipal wealth (McLaughlin et al., 2002; McLaughlin and Cooper, 2010), loss of urban versus agricultural land value (e.g. Snoussi et al., 2008; Sterr, 2008), and a community's social vulnerability to natural hazards (Cutter et al., 2003). Devoy (2008) added another perspective to coastal vulnerability due to SLR by means of the costs of coastal protection.

Here in this study, coastal vulnerability refers to geophysical vulnerability and is used to distinguish the integrated coastal behavior considering both negative and positive responses to climate change-induced conditions (i.e., resilience and susceptibility). Vulnerability assessment studies classify coastlines differently from strictly quantitative to semi-quantitative, non-adaptive to perfectly adaptive, science-driven to policy-driven, and simplistic to sophisticated, etc. (Fussel and Klein, 2006). In this study, CVI is based on the previous studies (Gornitz, 1991; Shaw et al., 1998; Thieler and Hammar-Klose, 2000; and Lopez et al., 2016), because of their efficiency and wide and large spatial scale use. They use similar physical variables and permit to assess vulnerability just associated to physical impacts of erosion and inundation. It is aimed to compare the sensitivity of each selected study for the regional characteristics due to differences in each ranking system, and then select the most robust one to guide coastal managers on decision making process. This analysis is applied to a coastal stretch characteristic of sensitive human-influenced Mediterranean coastline conditions, i.e. the Barcelona coastal region.

2. Study area

The Barcelona coast is located in the NE Spanish Mediterranean and it extends about 100 km around Barcelona city (Fig. 1). This stretch is representative of highly developed areas of the Mediterranean coastal zone, with large urban settlements and intensive use of the coastline for leisure and tourism, and as a consequence accumulating human-induced pressures, which make this a high sensitive and vulnerable coastline which has experienced an increase in coastal damages during the last decades (Jiménez et al., 2012). This area concentrates about 75 percent of the Catalan population and about the 52 percent of the Catalan GNP (see e.g. Jiménez et al., 2017).

It is a wave-dominated coast, comprising more than 100 beaches

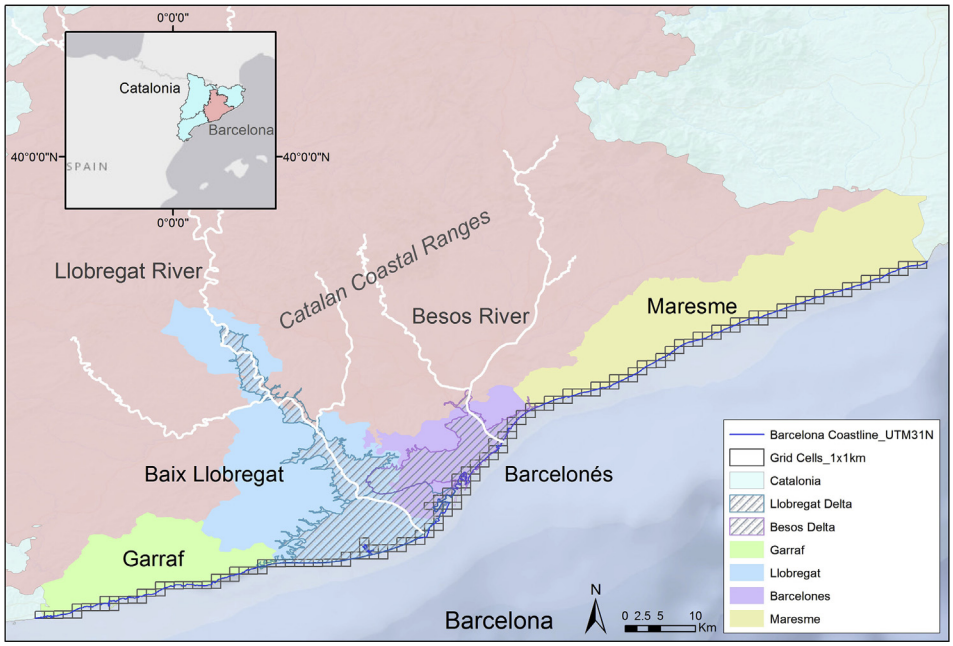

Fig. 1. Study area map and shoreline grids created in ArcGIS 10.5.1.

along 4 coastal comarcas (administrative units); Maresme, Barcelonès, Llobregat, and Garraf (Fig. 1).The beaches are characterized by coarse sand sediment northwards of Barcelona ($d_{50} \geq 0.4$ mm) whereas south of the Barcelona harbor they are composed by fine sediments ($d_{50} \geq 0.2$ mm) (Jiménez and Valdemoro, 2019). While about 65% of the Catalan beaches are retreating under current conditions (Jiménez and Valdemoro, 2019), the study area includes some of the most eroding beaches, the Maresme coast, with an average evolution rate of about -0.7 m/y and eroding stretches retreating at an average rate of -1.5 m/y (Jiménez and Valdemoro, 2019). This coastal stretch supports an important infrastructure network, being a coastal railway connecting Barcelona with northern small cities the most important one. This infrastructure is sensitive to storm-induced events in such a way that under the impact of extreme storms, the service can be disrupted (e.g. Ballesteros et al., 2018b; Jiménez et al., 2018). On the other hand, the city waterfront is composed by a set of artificial beaches which were built after the 90's and that, currently, support an intensive recreational use during all over the year. As an example, according to the Municipality of Barcelona, these beaches received more than 4.7 million of visitors during 2016. The Llobregat sector comprises deltaic beaches southward of Barcelona harbor with an area of natural interest at the Eastern part, and of residential and recreational interest at the Western end. Finally, the Garraf sector includes pocket beaches with a dominant recreational use.

3. Material and methods

The data used in this study to assess coastal vulnerability included in the corresponding indicators such as geomorphology and geology, the coastal slope of the region, sea level change, shoreline change, significant wave height, and tidal range. All the required data have been stored and manipulated within a geographic information system (Table 1).

The historical data sets for each variable are implemented as attribute tables, and vulnerability scores are calculated according to each selected methodology.

The recent coastline is trimmed from the original, projected ED50 and freely available European coastline shape file (EEA, 2017) and used with the Universal Transverse Mercator projection. After that, the coastline is divided into 160 cells of 1 km by 1 km comprising a grid template using ArcGIS10.5.1.

Variables are categorized on a scale of 1–5 (low risk to high risk) by breaking the range into five equal divisions (Table 2). Beside the geospatial comparison of varying vulnerability classes, the vulnerability class distributions are evaluated by using statistical analysis (skewness and mean). In this context, the cell distribution around moderate vulnerability classes (mean) and their peaks or extreme vulnerability categories are analyzed.

3.1. The CVI and its components

CVI studies addressing geophysical vulnerabilities are mostly adapted from Gornitz (1991) and the basic of physical–geological parameters include SLR, geomorphology, coastal slope and regional elevation, shoreline change, significant wave height, and tidal range. Geomorphological landforms represent resistance to erosion, where the rates of erosion are considered indicators of sensitivity to coastal processes. Wave energy is related to capacity for erosion, where relief and vertical land movements are considered indicators of inundation risk.

The selected methods and their ranking table comparisons are summarized in Table 2.

3.1.1. Geomorphology and geology

The morphology of the coast plays a pertinent role in determining the response of the coast to SLR, as it expresses the relative erodibility and the degree of resistance of the different landforms varying from high cliffs to sandy shores (Thieler and Hammar-Klose, 1999).

Geology or, namely, a rock-type variable, is associated with erodibility risk. Bedrock lithology, shore materials, and coastal landforms vary substantially in terms of their resistance to erosion. A generalized scale of lithologic and geomorphologic resistance to erosion was discussed by Gornitz and Kanciruk (1989).

The geomorphology analysis of the Catalan coast shows the major landforms of Barcelona's coastline. Sediments along the Barcelona city coast originated from the Besòs delta and the Llobregat emerged deltas, which are separated by the Barcelona Coastal Plain and are bounded by the Catalan Coastal Ranges to the north (Fig. 1). Maresme, extending from the city of Barcelona to the north is formed by the Tordera delta coast (Jiménez et al., 2018). The Besòs delta is limited by the Littoral Ranges to the north, and by the Barcelona Coastal Plain to the west,

Table 1
Data sources used in CVI calculations in this study.

Physical & Geological Variables		
Variable	Data Source	Data Period
Geomorphology/Geology	Cartographic and Geological Institute of Catalonia | Base Geologic 1:50,000	2007
Coastal Slope	Cartographic and Geological Institute of Catalonia | DEM 2 × 2	2016
Sea level change	Puertos del Estado (State Spanish Port System)	1993–2016
Shoreline change	Deltares strategic research program Coastal and Offshore Engineering	2004 & 2016
Significant wave height	Puertos del Estado (State Spanish Port System)	1958–2016
Tidal range	Puertos del Estado (State Spanish Port System)	1993–2016

which separates the Besòs delta from the neighboring Llobregat delta. It is a Holocene depositional system that was also active during the Pleistocene (or Ice Age). On the other hand, Barcelona city area is characterized by artificial beaches and a big harbor that extends along more than 15 km. Its southern part developed over the delta plain of the Llobregat River, which create a sandy coastline over 18 km long. Additionally, in the south, the Garraf coast is characterized by the low calcareous cliffs (Ojeda and Guillén, 2008).

A detailed digital geomorphological map is made by using digitized raster topographic sheets of 1:50,000 scale (Table 2), provided by the Cartographic and Geological Institute of Catalonia (ICGC, 2017). A geological map of the Besòs delta and adjacent zones is digitized at scale of 1:50,000 derived from the data sources of the Instituto Geológico y Minero de España (IGME, 2017). The delta is being constituted by sediments supplied by the Besòs River and their tributaries.

The digitalized geomorphological map is then attributed into the 1 km × 1 km grid cells, so that each cell has its own unique value to be evaluated in selected CVIs with varying values.

3.1.2. Coastal slope and regional elevation

The coastal slope is an indicator of not only the relative risk of inundation, but also the potential speed of shoreline retreat. Thus, on a steep coast, the consequence of SLR would be insignificant, which is on the contrary to a gentle sloping coast, where any rise in sea level would inundate large extents of land (Nageswara Rao et al., 2008).

While the elevation zone within 1 m of the shoreline faces the highest probability of permanent inundation, the coastal strip within 5 m of the present shoreline is also at high risk to above the normal tides from severe storm surges. Gornitz (1991) stated that the hazard decreases progressively for higher average elevations. In any case, it has to be considered that storm surges along the Catalan coast are not especially relevant, being the wave-induced run-up, the most important component contributing to storm-induced total water level (Mendoza and Jiménez, 2009).

The emerged coastal slope of Barcelona's coasts is calculated by using the orthometric height of the Digital Elevation Model (DEM), which is based on the altimetry information of the topographic base of Catalonia 1:5.000 provided by the ICGC (2017) (Table 1). The DEM of the region is regenerated with using a 2 m × 2 m regular grid model provided in and reconfigured as 10 × 10 m tiles, then it is mosaicked in GeoTIFF format in ArcGIS 10.5.1. The mosaic tool is useful when two or more adjacent raster datasets need to be merged into one entity. Some mosaic techniques can help minimize the abrupt changes along the boundaries of the overlapping raster.

After the mean regional elevations are calculated, the slopes are calculated along the coastline. The slope values are characterized with 1 km × 1 km grid cells, varying from 1 or 2 to 95 percentiles. The obtained data indicates that the regional elevations vary from a few meters to 80–90 m respectively. Spatial aggregation of values into 1 km grids results in relatively mild slope coastal profile.

3.1.3. Sea-level change

The relative sea-level change variable is derived from the increase (or decrease) in annual mean water elevation over time as measured at tide gauge stations along the coast (e.g., Emery and Aubrey, 1991). This variable inherently includes both the global eustatic SLR as well as local isostatic and tectonic land motion (subsidence). Duro et al. (2004) reported that there are rich soft sediments in pore water and organic matter in Llobregat delta plain, with average subsidence rates of 1.25 mm yr^{-1}, and 6 mm yr^{-1} as a maximum value. Relative sea-level change data is a historical record, and thus it shows changes for only recent time scales (the last 50–100 years).

The Barcelona tide gauge data set starting from 1993 to 2016 is also used as the primary source of information for sea level trends in the study area. The tide gauge is placed at the dock 140 of the ENAGAS building at 2.17° E, 41.34° N coordinates (Fig. 2). The historical data set is downloaded from Puertos del Estado (Table 2) (Puertos del Estado, 2017).

3.1.4. Shoreline change

Coastlines are in different types of coastal landforms including beaches, tidal flats, deltas, cliffs, and barrier islands with varying responses to erosion/accretion. Erosion and accretion patterns indicate the dynamics of the coast. In CVI methodology, shoreline change is used as an indicator for the potential impact of climate change, and it can be considered as a resilience capacity of the coast.

Similar with most of the beaches in Mediterranean Sea, Barcelona beaches are associated with both natural processes and human-induced actions (Ojeda and Guillén, 2008). The sedimentary shorelines are subject to natural, dynamic processes such as the southwards directed net longshore sediment transport (CIIRC, 2010; CEDEX, 2014; Jiménez and Valdemoro, 2019).

The shoreline change is calculated here based on the shoreline records of 2004 and 2016 (Luijendijk et al., 2018). Digitized shoreline records are calculated using the Digital Shoreline Analysis System (DSAS) tool of Arc-GIS developed by U.S. Geological Survey. The DSAS is an extension that enhances the normal functionality of ESRI ArcGIS software. DSAS uses a measurement baseline method (Leatherman and Clow, 1983) to calculate rate-of-change statistics for a time series of shorelines. The baseline is constructed and served as the starting point for all transects cast by the DSAS application. Transects intersect each shoreline at the measurement points that are used to calculate shoreline-change rates (Thieler et al., 2009). Transects are placed at 100-m intervals along the shoreline stretch, either landward or seaward, and perpendicularly to the baseline. Shoreline change (m/yr) is then analyzed to derive the rate of shoreline change over time by using the End-Point Rate (EPR) technique. The major advantages of the EPR are the ease of computation and the minimal requirement of only two shoreline dates (Thieler et al., 2009).

Representing positive or negative values due to natural processes are then shown as EPR results, indicating accretion or erosion rates. After that, the results are spatially aggregated at a 1 km grid cell scale and attributed to each grid cell respectively.

3.1.5. Significant wave height

The waves are the main hydrodynamic force on the beaches,

Table 2
Comparison of several CVI's for varying ranking values.

						Coastal Vulnerability Index Ranking				
		CVI Reference				Very Low	Low	Moderate	High	Very High
Variable	Unit	Lopez et al., 2016	Thieler and Hammar-Klose, 2000	Shaw et al., 1998	Gornitz, 1991	1	2	3	4	5
Geomorphology	-	X				Rocky/ hard cliffs (little erosion)	Embank-ments	Cliffs subject to erosion, Vegetative shores (pond or lake type)	Soft shores (beach rocks), Soft shores (mine-waste sediment), Soft shores (heterogeneous category grain size)	Small beaches, Developed beaches, Soft, non-cohesive sediments, Artificial beaches, Soft beaches (uncertain category grain size)
	-		X		X	Rocky, cliffed coasts, Fiords, Fiards	Medium cliffs Indented coasts	Low cliffs, Glacial drift, Alluvial plains	Cobble beaches, Estuary Lagoon	Barrier beaches, Sand beaches, Salt marsh, Mud flats, Deltas, Mangroves, Coral reefs,
Land form	-			X		Fiords, high rock cliffs, Fiards	Moderate and low rock cliffs	Beach, unconsolidated sediment over bedrock	Barrier, bluffs, salt marsh, peat, mud flat, delta, tombolo	Ice-bonded sediment, Ice-rich sediment, Ice shelf, Tidewater glacier
Coastal slope	%	X				> 12	8-12	4-8	2-4	<2
	%		X			> 1.9	1.3 – 1.9	0.9 – 1.3	0. 6 - 0.9	< 0.6
Relief	m			X	X	>30	21-30	11-20	6-10	0-5.0
Relative sea-level change	mm/yr	X					0.0-1.5	1.5-3.9	3.9-9.7	> 9.7
	mm/yr		X			< -1.21	-1.21 – 0.1	0.1 – 1.24	1.24 - 1.36	> 1.36
	mm/yr			X		> -5.0	-5.0 to -2.0	-19 – 2.0	2.1 to 4.0	>4.0
	mm/yr				X	< -1.0	-1.0-0.9	1.0-2.0	2.1-4.0	> 4.0

						Very Low	Low	Moderate	High	Very High
		CVI Reference								
Variable	Unit	Lopez et al., 2016	Thieler and Hammar-Klose, 2000	Shaw et al, 1998	Gornitz, 1991	1	2	3	4	5
Shoreline erosion/ accretion	m/yr	X				> + 1.0		-1.0 - +1.0		< - 1.0
	m/yr		X		X	> 2.0	1.0 - 2.0	-1.0 - +1.0	-1.1 - -2.0	< - 2.0
Shoreline displacement	m/yr			X		> + 0.1	0.0	-0.1 - -0.5	-0.6- -1.0	>-1.0
Mean tide range	m	X	X			> 6.0	4.1 - 6.0	2.0 - 4.0	1.0 - 1.9	< 1.0
	m			X		<0.50	0.5-1.9	2.0 - 4.0	4.1-6.0	>6.0
	m				X	<1.0	1.0-1.9	2.0-4.0	4.1-6.0	>6.0
Wave climate	$Hs_{95}^2/Hs_{threshold}^2$	X				< 0.65	0.65 - 0.75	0.75 - 1.0	1.0 - 1.5	> 1.5
Mean wave height	m		X			< 1.1	1.1 – 2.0	2.0 – 2.25	2.25 – 2.60	> 2.60
Maximum wave height	m			X	X	0-2.9	3.0-4.9	5.0-5.9	6.0-6.9	>6.9
Geology					X	Plutonic, Volcanic, High-medium grade metamor-phics	Low grade metamor-phics, Sand-stones and conglo-merates,	Most sedimen-tary rocks	Coarse, poorly sorted, unconsolidated sediments	Fine, consolidated sediment, Ice
Rock Type				X		Plutonic rocks, high-grade metamor-phic & volcanic rocks	Metamor-phic rocks	Most sedimen-tary rocks	Poorly consolidated sediment	Unconsolidated sediment, Ice

transforming the shoreline by sediment transport. Waves with larger wave height are broken with higher energy on beaches and mobilize larger sediment volumes and induce larger morphodynamic changes. Thus, the increase in the incident wave power, particularly if it is combined with an increased sea level, catalyze many coastal responses such as erosion and inundation. Hence, they have vital consequences in terms of coastal geomorphology. Therefore, in CVI applications, wave height, is included as an indicator of wave energy, driving coastal

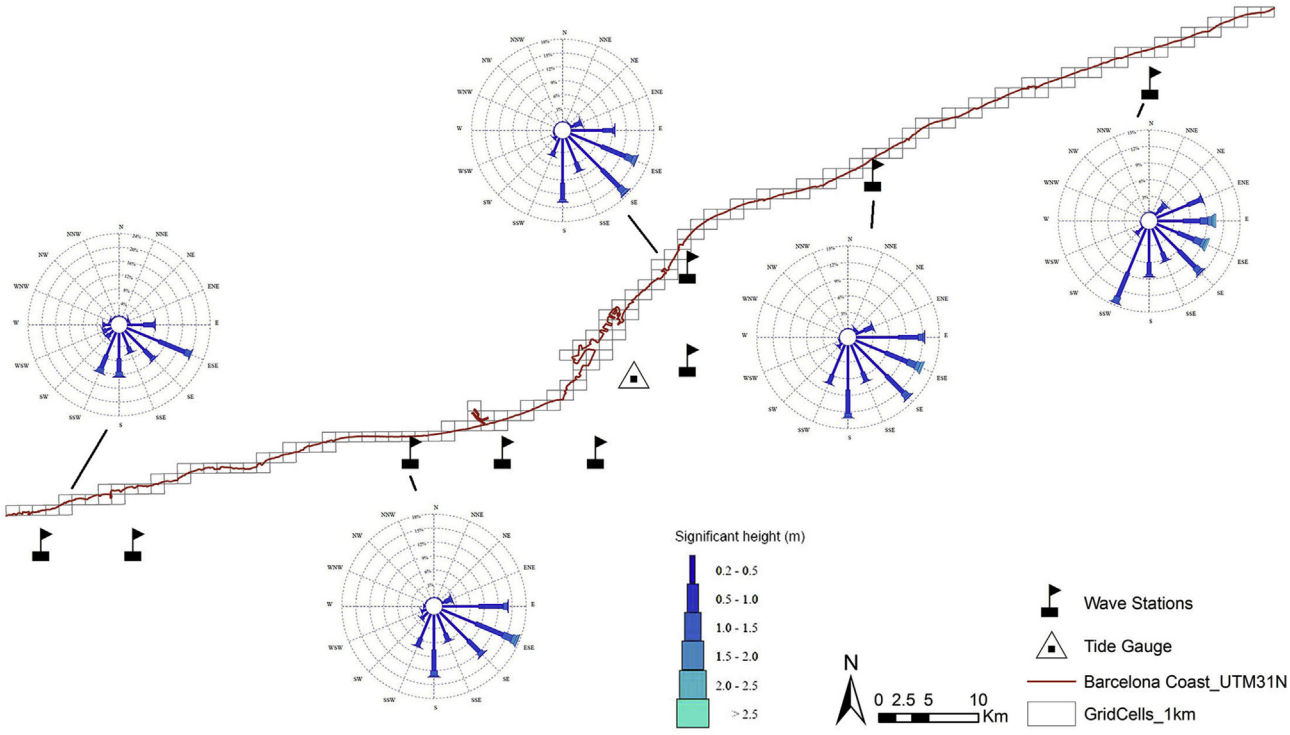

Fig. 2. Wave stations, tide gauges, and wave rose samples along the coastline.

sediment budget.

To account this effect of wave power, Lopez et al. (2016) proposed to use a variable indicating the power content instead of using a single dependence on wave height as mots of CVI usually does. They proposed to use the formula (Equation (1)) to define the storm erosion-induced coastal vulnerability.

$$\frac{Hs_{95\%}^2}{Hs_{threshold}^2} \quad (1)$$

In this study, wave data along the coast was obtained from the official online website of Puertos del Estado (Ports of the State) for the period of 1958–2016 (Puertos del Estado, 2017).

$H_{s95\%}$ = 95th percentile wave height along the coast
$H_{s\ threshold}$ = locally adopted threshold for storm definition

According to the data, the mean significant wave height varies between 0.45 m and 0.6 m whereas the maximum significant wave height was 5 m. The corresponding mean wave period was about 4.5 s. Fig. 2 shows the directional distribution of wave conditions along the study area for the available data.

The total H_s along the Catalan coast shows a gradual decrease from north to south and the main direction of the wave energy gradually turns from north to northeast, east, southeast, and finally to the south (e.g. Bowman et al., 2009).

3.1.6. Tidal range

The tidal range is linked to both the permanent and episodic inundation hazards. Gornitz (1991) suggests that a high tidal range is associated with stronger tidal currents, which have the capacity to cause the erosion and transportation of sediment in such a way that, macro-tidal coasts (> 4 m) will be more vulnerable than those with smaller values. Similarly, Shaw et al. (1998) modifying Gornitz (1991) added that an increase in the mean water level would increase the flooding frequency of high intertidal environments, such as deltas and estuaries. This will also result in the flooding of areas presently above astronomical high tide levels. According to the perspective of both Shaw et al. (1998) and Gornitz (1991); a coastal area is considered highly vulnerable if it experiences a high tidal range, whereas those with low tidal ranges are designated to be of low vulnerability.

Thieler and Hammar-Klose (2000) classified micro-tidal coasts to be of high vulnerability and macro-tidal coasts to be of low vulnerability. The reason behind this argument is that, on micro-tidal coasts, the sea level is always quite close to high tide; therefore, in the event of a storm surge, flooding is more likely than at macro-tidal coasts (Pendleton et al., 2004). On the other hand, at macro-tidal coasts, it is not unlikely that the sea level during a storm surge event is significantly lower than the high-tide level, thus increasing the possibility of reduced flood risk (Rosen, 1977).

Tidal range values of the study area are obtained in the tide tables from the tide gauge placed at the dock 140 of the ENAGAS building at 2.17° E, 41.34° N coordinates. The historical data set is downloaded from Puertos del Estado (Table 1) (Puertos del Estado, 2017). The Catalan coast is micro-tidal, with a range of 0.2 m. The tidal range variable has been assigned a mid-value rank; all 160 cells have been assigned the same value within this study area, which is 0.23 m.

3.2. CVI calculations

One of the initial methods to evaluate the potential vulnerability has been broadly adapted from Gornitz (1990, 1991), who used the U.S. coastline on a national scale by focusing on seven variables that strongly influenced coastal evolution. The overall CVI is described as the square root of the product of the variables divided by the number of variables (n).

a_4 = shoreline change rates
a_5 = significant wave height
a_6 = tidal range
a_1 = geomorphology
a_2 = coastal slope/relief
a_3 = relative sea level rate

$$CVI = \sqrt[2]{\frac{a_1 * a_2 * a_3 * a_4 * a_5 * a_6}{n}} \quad (2)$$

Here, Python scripts(Python Software Foundation) for each ranking table are created to assign the vulnerability classes of each variable within the ArcGIS spatial calculation tool with respect to their threshold values for each category. Vulnerability levels of each variable are classified from 1 (very low vulnerability) to 5 (very high vulnerability), according to the variable ranking tables of the corresponding study.

The vulnerability class values are used in Equation (2) to calculate the composite CVI value for all the different coastal stretches that combine to form the national coastline. Subsequently, the vulnerability categories are represented with percentile ranges as 0–25%, 25–50%, 50–75%, and 75–100% (Thieler and Hammar-Klose, 2000; Shaw et al., 1998). In other words, a value of 1 represents the lowest vulnerability and where the value of 4 represents the highest vulnerability.

The distribution of vulnerability classes of cells are then examined with statistical analysis by way of skewness and the mean values of each study to examine the reason behind the difference of the assigned vulnerability classes and to help with selecting the most realistic approach for future planning.

4. Results

4.1. Physical and geomorphological parameters

4.1.1. Geomorphology and geology

The Maresme coast is an almost rectilinear sedimentary coastline which is only interrupted by several marinas. Next, the Barcelona city area is characterized by artificial beaches and a big harbor that extend along more than 15 km. Its southern part developed over the delta plain of the Llobregat River, which creates a sandy coastline over 18 km long. Additionally, in the south, the Garraf coast is characterized by the low calcareous cliffs (Ojeda and Guillén, 2008). Fig. 3-a depicts the geomorphological component of analyzed CVIs.

Although the geology of Garraf, for instance, is mostly dominated by the cliffs, spatial aggregation of adjacent series of pocket beaches within 1 km grid dominate the geomorphological character mostly as sandy beaches. This leads to the following assigned vulnerability rankings: 74 percent of the grids are sand, 11 percent is cobble, 11 percent is Portland, and 4 percent is cobble beach and low cliffs.

Gornitz (1991), Shaw et al. (1998), Thieler and Hammar-Klose (2000) and Lopez et al. (2016) indicate similar vulnerability with respect to geomorphology. The classification due to geomorphological characteristics indicates that 74 percent of the coastline is very highly vulnerable, while 11 percent is highly vulnerable, 0.6 percent is moderately vulnerable, 11.4 percent is at a low level of vulnerability, and 3 percent has a very low vulnerability level. The green grid cells are showing where the coastline is composed by the Barcelona Port.

Further, regarding the geomorphology variable, only Shaw et al. (1998) and Gornitz (1991) added the geology variable to be included in the calculations of the overall CVI. Fig. 3-b is showing how the region's rock type contributes to overall vulnerability. The composition of the passive (rigid) part of the Catalan coast is clearly dominated (about 83%) by the natural component (cliffs and rocky coasts), with the exception of Maresme (coast northwards of Barcelona), where the rigid coastline is essentially human-built (revetment protecting the coastal railway and other coastal protection structures). According to their ranking systems, both agreed that most of the coastline of the Barcelona province is highly vulnerable with respect to the coasts' resistance to inundation by SLR. According to the calculations and their ranking categories, 81 percent of the stretch is highly vulnerable (namely, in Barcelones, Maresme, and Garraf municipalities), 10 percent of the cells are moderately vulnerable, 1 percent of cells are at a low vulnerability level, and 8 percent of cells are at a very low level of vulnerability due to their geological characteristics. The calculations also show that compared to three other coastal comarcas, Llobregat is moderately vulnerable to SLR due to the geological characteristics of the coast.

4.1.2. Coastal slope and regional elevation

Shaw et al. (1998) and Gornitz (1991) used regional elevation parameters to characterize the vulnerability of coastal regions due to inundation, while Lopez et al. (2016) and Thieler and Hammar-Klose (2000) prefer to define this variable as coastal slope.

Coastal slope and regional relief variable ranking comparisons for Barcelona's coast are shown in Fig. 4. In this figure, Shaw et al. (1998) and Gornitz (1991) both indicate similar vulnerability classes due to the elevation characteristics of the region. According to the calculations, 87 percent of the cells are very highly vulnerable, 6 percent are highly vulnerable, 2 percent are moderately vulnerable, 1 percent are at a low level of vulnerability, and 4 percent are at a very low vulnerability level due to relief variables. On the other hand, spatial distribution of the vulnerability levels indicates that, according to their ranking categories, Shaw et al. (1998) and Gornitz (1991) depict the whole coastline as inherently highly vulnerable. This conclusion holds in areas, with the exception of the coasts of some municipalities of Garraf; such as Vilanova i la Geltrú and Sitges, and the municipalities of Maresme, such as Vilassar de Mar and Cabrera de Mar.

On the other hand, Lopez et al. (2016) and Thieler and Hammar-Klose (2000) indicate similar vulnerability classes due to a coastal slope with relatively higher category values. The calculations made within this ranking classification shows that according to Lopez et al. (2016),

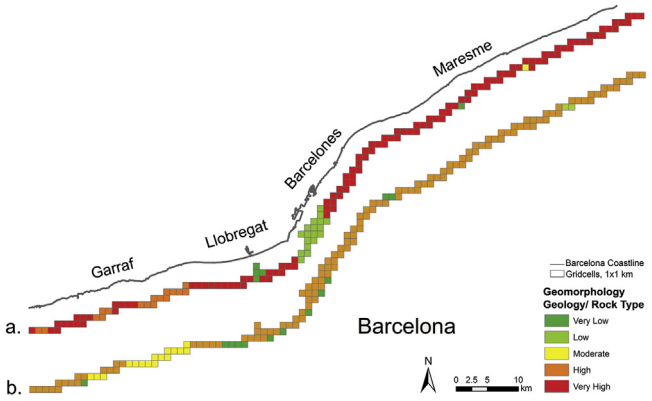

Fig. 3. Geomorphological component of analyzed CVIs: a. Lopez et al. (2016); Thieler and Hammar-Klose (2000); Shaw et al. (1998), and Gornitz (1991); b. Geological comparison for CVIs: Shaw et al. (1998) and Gornitz (1991).

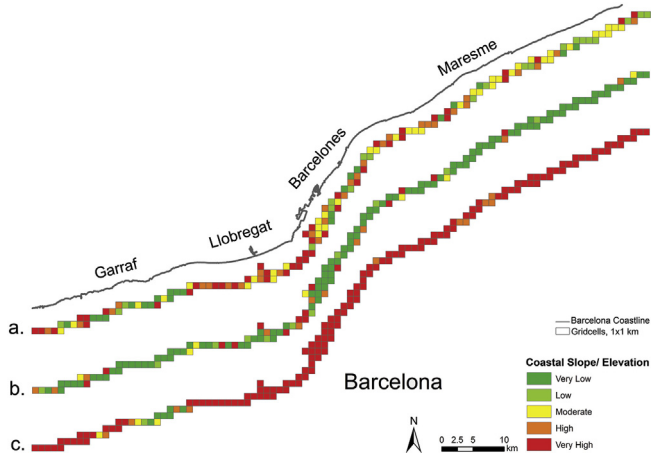

Fig. 4. Coastal slope and relief component of analyzed CVIs: a. Lopez et al. (2016); b. Thieler and Hammar-Klose (2000); c. Shaw et al. (1998) and Gornitz (1991).

14 percent of the total grid cells are very low vulnerable, 13 percent are low vulnerable, 26 percent are moderately vulnerable, 19 percent are highly vulnerable, and 28 percent are very highly vulnerable due to the coastal slope variable. While in the calculations of Thieler and Hammar-Klose (2000), 73 percent of the grid cells are very low, 7 percent are low, 4 percent are moderate, 7 percent are very high, and 9 percent are very high vulnerable due to the emerged coastal slope of the region.

Essentially, if these variables are analyzed separately as coastal slope and coastal elevation, it can be relatively easier to define the huge difference. Although the coastal slope and coastal elevation are basically representing a similar approach, the coastal slope in fact represents the ratio between the emerged elevation and the width of the coast.

Although Lopez et al. (2016) and Thieler and Hammar-Klose (2000) use the same variable, namely coastal slope, the ranking values of Lopez et al. (2016) represent more conservative ranges than compared to Thieler and Hammar-Klose (2000), which indicate higher vulnerability. Consequently, the same mild, shore-face slope values point out higher vulnerable scores from Lopez et al. (2016) compared to Thieler and Hammar-Klose (2000).

On the other hand, Shaw et al. (1998) and Gornitz (1991) define the inundation risk by the elevation of the land. In this case, due to the selected rank proposed by these authors, the Barcelona coast scored as having a very high level of vulnerability.

4.1.3. Sea level change

The sea level change variable for coasts of the Barcelona province does not show any variances spatially, since the data is retrieved from the same data station along the shoreline and this variable usually presents a small spatial variation unless that the area of study is really large. Fig. 5 is showing the relative SLR comparison for the four selected ranking classes.

As seen from Fig. 5, grids of “a” (representing Lopez et al., 2016) indicate a moderate vulnerability class with an assumption of SLR of 0.18–0.38 m corresponding to RLSR of 1.5–3.9 mm annually, which is a relatively low value. According to the ranking table of Thieler and Hammar-Klose (2000), Barcelona coasts are very highly vulnerable to relative SLR (Fig. 5-b). On the other hand, based on the ranking tables of both Shaw et al. (1998) and Gornitz (1991), the shoreline is highly vulnerable to SLR (Fig. 5-c).

4.1.4. Shoreline change

The adapted values of Shaw et al. (1998) for shoreline changes differ from the ranges used by Gornitz (1991) and Thieler and Hammar-Klose (2000), because some of Canada's coasts experience extensive,

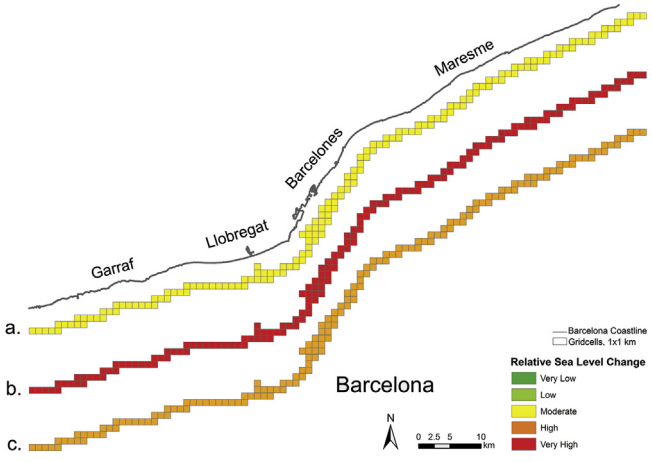

Fig. 5. Relative SLR component of analyzed CVIs: a. Lopez et al. (2016); b. Thieler and Hammar-Klose (2000); c. Shaw et al. (1998) and Gornitz (1991).

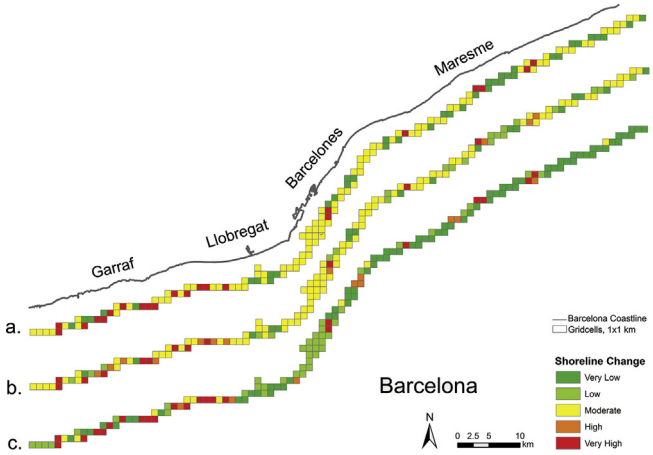

Fig. 6. Shoreline change component of analyzed CVIs: a. Lopez et al. (2016), b. Thieler and Hammar-Klose (2000); and Gornitz (1991); c. Shaw et al. (1998).

persistent erosion, but average rates are less than 1 m annually (Table 1). Most rocky coastlines are assigned a rate of 0 m annually, although very slow recession commonly occurs. Fig. 6 is showing the shoreline change comparison for varying ranking values for selected CVIs for the study area. As seen in the figure, Thieler and Hammar-Klose (2000); Gornitz (1991), and Lopez et al. (2016) have slight differences in shoreline change due to ranking values. Thus, the main difference is observed between Thieler and Hammar-Klose (2000) and Shaw et al. (1998).

In this context, it can be easily said that the approach of Thieler and Hammar-Klose (2000) on shoreline change is more conservative than that of Shaw et al. (1998), especially for the northern part of the province. On the other hand, they are all agreed on the high vulnerability scale, especially for the Garraf and Sitges shores located in the southern part of Barcelona. Unlike other applications of the CVI rankings, which considered five shoreline evolution categories, here, and the above three behavioral types were directly assigned by Lopez et al. (2016): very low, moderate, and very high vulnerability classes as shown in Table 1.

In these comparisons, the vulnerability categories of Lopez et al. (2016) are listed as very high, moderate, and very low. According to their rankings, 14 percent of the shoreline in grid cells is at a very high risk, 61 percent of the shoreline has a moderate erosion risk, and 25 percent of shoreline is at a high erosion risk.

Since Thieler and Hammar-Klose (2000) is adapted from Gornitz (1991), they agreed on the vulnerability levels. Eventually, according to their ranking categories, 8 percent of the shoreline in grids has very high vulnerability, 7 percent is highly vulnerable, 60 percent is moderately vulnerable, 14 percent is at a low level of vulnerability, and 11 percent is at a very low erosion risk. On the other hand, the results of Shaw et al. (1998) show a more flexible evaluation on erosion vulnerability of Barcelona's coasts respectively. Due to their ranking classes, 14 percent of the stretch has very high vulnerability, 6 percent is highly vulnerable, 6 percent is moderately vulnerable, 26 percent is at a low level of vulnerability, and 48 percent of the coast has a very low vulnerability level.

When it is evaluated spatially, all of the CVIs shoreline change vulnerability classifications indicate grids of relatively low vulnerability, especially for the municipalities of Maresme (except a few grid cells). However, Ballesteros et al. (2018) indicates the medium-term shoreline displacement rate along the northwards of Barcelona, namely the Maresme coast, and highlights that the coastline is mostly eroding, particularly downcoast of ports, as expected. The difference between the relatively low vulnerability ranking values is mostly due to the weighted average values of 100 m transects contributing to each 1 km coastline cell.

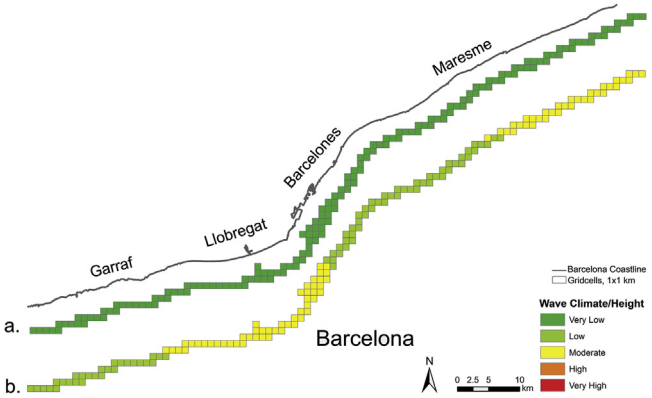

Fig. 7. Wave height and wave climate component of analyzed CVIs: a. Lopez et al. (2016); Thieler and Hammar-Klose (2000); b. Shaw et al. (1998); and Gornitz (1991).

4.1.5. Significant wave height

Fig. 7 shows the attributed values for the wave height and wave climate in the grid cells. Maximum and mean wave height values are gained from 10 wave stations that represent the wave climate along the shoreline. The reports shows that the maximum wave heights are 5 m, while mean wave heights are 0.4–0.55 m. Therefore, the whole shoreline is in very low, low, and moderate risk classes for all selected CVIs.

The ranking classes for Lopez et al. (2016) and Thieler and Hammar-Klose (2000) indicate that the wave climate or mean wave height below 0.55–0.65 m has a very low level of vulnerability. In this context, the whole Barcelona coastline is representing a very low vulnerability level with respect to wave energy.

Conversely, the calculations based on rankings of Shaw et al. (1998) and Gornitz (1991) reveal that the maximum wave height values between 3.0 and 4.9 m are categorized as low vulnerability and values between 5.0 and 5.9 m are in the moderate vulnerability category. In this context, 52 percent of cells are in the moderate category and 48 percent of cells are categorized as in the low vulnerability category. In this context, the coasts of Llobregat and the northern municipalities of Maresme have moderate vulnerability levels and the municipalities of Garraf and Barcelones have a low vulnerability contribution to the overall CVI.

4.1.6. Tidal range

The Catalan coast is micro-tidal, with a range of less than 0.2 m, where the tidal range can be considered negligible. The comparison of the tidal range of Barcelona's coastline for the ranking value of various authors is given in Fig. 8. Similar to sea-level records, the tidal records originate from one data station along the Barcelona province.

As seen in Table 2, Lopez et al. (2016) and Thieler and Hammar-Klose (2000) claim that vulnerability evaluations for the coast rank at very highly vulnerable level due to the tidal effect, while Shaw et al. (1998) and Gornitz (1991) claim a very low level of vulnerability. The ranking tables of Lopez et al. (2016) and Thieler and Hammar-Klose (2000) agree that all the grid cells of shore contributions to the overall CVI have a value of five (very high tidal vulnerability), while Shaw et al. (1998) and Gornitz (1991) considered the contribution of the tidal effect on the overall CVI as having a value of one (a very low vulnerability level).

Gornitz (1991) emphasized that a coastal area with a high tidal range is considered highly vulnerable, whereas those with a low tidal range are designated to be of low vulnerability.

Contrary to Gornitz (1991), Thieler and Hammar-Klose (2000) defines the tidal vulnerability relating the impact of a tidal range with the potential influence of storms on coastal evolution. They explain the relationship as a 50 percent chance of a storm occurring above mean tide. Consequently, according to their evaluations, a micro-tidal coastline is essentially always near high tide and, therefore, always at the greatest risk of significant storm impact.

4.2. The overall vulnerability classification along the coast

Fig. 9 is showing the overall ranking category distribution for the four selected modified ranking tables.

A vulnerability comparison due to percentile areal distribution for Thieler and Hammar-Klose (2000); Shaw et al. (1998); and Gornitz (1991), who all divided the overall CVI values into equal 4 percentage classes, is summarized in Fig. 10. Originally, Lopez et al. (2016) divided the overall CVI values into five equal classes. However, in this study the overall vulnerability classes of Lopez et al. (2016) are distributed over 4 equal percentage classes to compare with the other selected CVIs.

The distribution of vulnerability classes of cells are then examined through statistical analysis by means of skewness and mean values of each study to examine the reasons behind the differences of the assigned vulnerability classes and help to select the most realistic approach for future planning.

In this context, a further characterization of the number cell distribution among the vulnerability classes is explained using skewness, mean and maximum values (Table 3). These basic statistical terminology explains how the cells are distributed around sample mean (skewness) or in other words among the low and very high vulnerability classes.

Skewness is negative for a distribution in which the data are spread out more to the left for Lopez et al. (2016) and Gornitz (1991). That means the distribution of vulnerability categories to the left shifted,

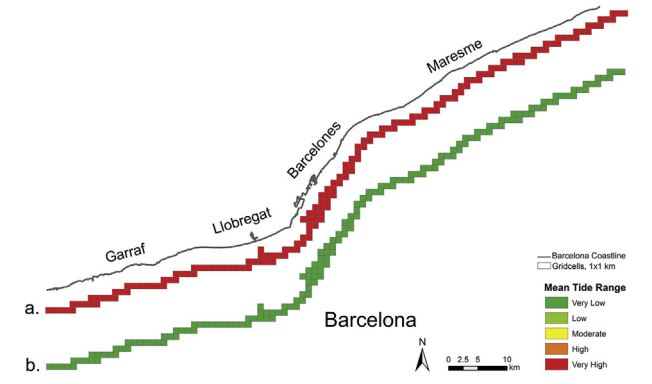

Fig. 8. Tidal range component of analyzed CVIs: a. Lopez et al. (2016) and Thieler and Hammar-Klose (2000); b. Shaw et al. (1998) and Gornitz (1991).

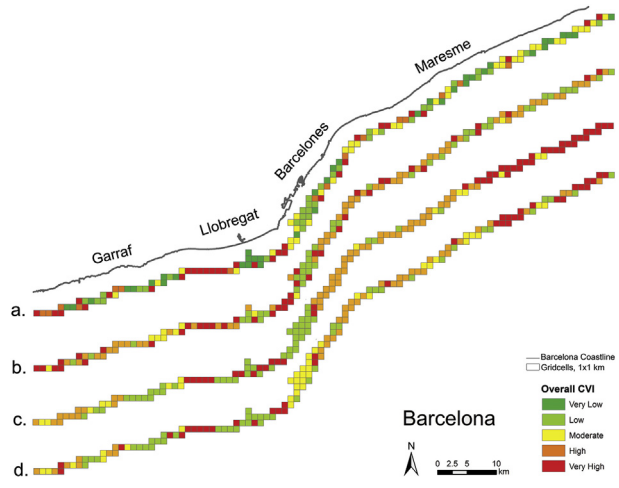

Fig. 9. The overall CVI ranking distribution (a: Lopez et al., 2016; b: Thieler and Hammar-Klose, 2000; c: Shaw et al., 1998; d: Gornitz, 1991).

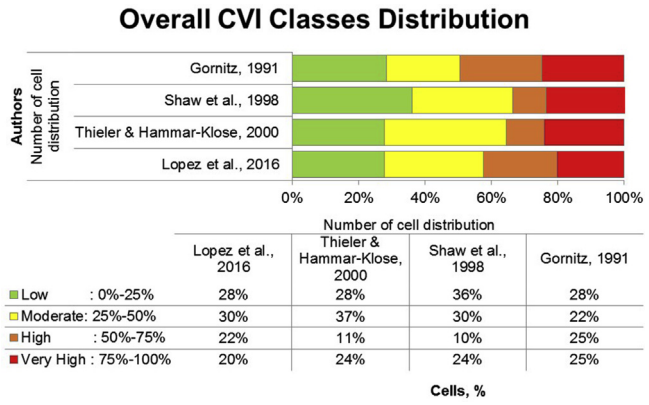

Fig. 10. The overall CVI ranking comparison for all authors.

indicating low vulnerability levels. However, the vulnerability distribution of Thieler and Hammar-Klose (2000) with highly skewed characters shows a higher moderate vulnerability level than the other authors (Table 3).

The high skewness supports the dense cell distribution around the moderate vulnerability class, which attempts the evaluation of high and low vulnerability classes diffused in the moderate class. This contains the risk of ignorance with respect to the highly vulnerable coastal stretch when decision makers plan action lists.

The spatial distribution of varying overall CVI categories and their statistical meanings are discussed in detail in the Discussion section.

5. Discussion

Besides the scientific popularity of usage and development of vulnerability index tools, CVIs are strong management tools to highlight potential coastal hotspots to a given set of climatic hazards. They efficiently simplify a number of processes acting at different scales, which should require applying robust and detailed modeling to fully characterize the induced coastal response. This permits to identify coastal hotspots to analyzed climatic hazards at regional scale which is a crucial step in long-term and large scale coastal planning to define coastal protection and adaptation strategies. However, this approach presents some uncertainties that can condition the representativeness of the obtained results and, in consequence, the effectiveness of adopted decisions. To tackle this problem from the practical standpoint, it has been made an analysis of the effect of selecting different versions of the index to be used and, they have been applied to a coastal stretch representative of urban Mediterranean coastlines.

Thus, in this study the vulnerability of the Barcelona coast is analyzed by comparing the sensitivity of four different versions of the CVI. They are based on the equation proposed by Gornitz (1991) which computes the vulnerability index as the square root of the product of the variables divided by the number of variables. Although there are some concerns about the potential error sources due to its tendency to distort the output range and distribution of the final (Gibb et al., 1992), this method is still widely used. Furthermore, Cogswell et al. (2018) claims that the method is sensitive to the number of variables used; more variables increase the skewness, and mean of the coastline index distribution at predictable rates and, to avoid such aspects they propose to use the geometric mean. However, as Cogswell et al. (2018) pointed out, that method also presents some shortcomings.

In this study, the four selected CVI versions include six to seven variables contributing to the overall scores, which are clustered in four vulnerability classes. In order to select the "best" one properly representing the relative vulnerability of the study area, it is crucial to analyze the bias and their sources. Consequently, here in this paper, the discussions on the sources of bias focus not only on the variables and their ranking table categories individually, but also on the statistical parameters of the overall CVI categorizations.

Geomorphology is the only variable that all the four CVI rankings categorized with the same vulnerability classes. This is due to fact that all of them consider the role played by this variable to control vulnerability in the same way. Moreover, as this variable is assessed in qualitative terms, i.e. coastal type, the associated ranking intervals are almost the same for the different methods.

With respect to the wave climate component, relatively small differences are detected among the different methods. This is due to the different definitions adopted to characterize the wave climate. Formally speaking, if this component is going to be used to characterize storm-induced risks, the use of the mean wave height should not be the best choice. In this context, the use of an extreme value such as the maximum wave height (Gornitz, 1991; Shaw et al., 1998) would be a more representative approach. In any case, the selected intervals to characterize the vulnerability associated to this component should be adapted to regional wave characteristics since they can significantly vary. In the case showed here it is recommended to adapt such range to the Western Mediterranean storm wave climate (Mendoza et al., 2011).

Although all methods consider shoreline evolution in the same way, they provide different vulnerability values due to differences in the ranking system. Again, the most realistic option will be to select a rank adapted to local conditions. This should consider not only the typical shoreline evolution rates in the area but, also the characteristic beach width. Thus, a given shoreline retreat will have not the same practical consequences in a narrow or a wide beach. Thus, this rank should be established taking into account regional statistics on shoreline changes and beach widths (Jiménez and Valdemoro, 2019), as well as the dominant beach uses which determine the optimum and minimum widths to be managed (e.g. Jiménez et al., 2017). Moreover, the way in which local values are spatially integrated may hide the real coastal vulnerability. When averaging the shoreline behavior within a sector, accretive sectors are artificially compensating erosive ones. However, in reality, this compensation does not exist and if a significant percentage of a given sector is erosive, it should be necessary to reflect it to properly identify the sector as vulnerable. This occurs along the Maresme coast where this way of integration hides the presence of severe eroding stretches (Ballesteros et al., 2018; Jiménez and Valdemoro, 2019).

Coastal slope and elevation assessment show a larges variation in vulnerability classes. For instance, Shaw et al. (1998) and Gornitz (1991) used coastal elevation to reflect the vulnerabilities due to SLR and storm surge. In this case study, their ranking category reveals that most of the Barcelona coastline is highly vulnerable. However, as it was previously mentioned, this is not directly applicable to the Barcelona case. As storm surge is not significant in this area, the storm-induced

Table 3
Statistical analysis results of CVI comparisons for all authors.

Authors	Skewness	Mean	Maximum Value	Skewness Comment
Lopez et al. (2016)	−0.74	8.66	51.03	moderately skewed
Thieler and Hammar-Klose (2000)	1.49	7.91	51.03	highly skewed
Shaw et al. (1998)	0.75	13.09	105.64	moderately skewed
Gornitz (1991)	−0.49	17.57	105.64	fairly symmetrical

inundation is mainly controlled by run-up. Thus, when assessing this risk factor by using inundation models, obtained results characterize this coast as relatively moderate to low vulnerable with few exemptions associated to the low-lying stretches such as the Tordera and Llobregat delta (Ballesteros et al., 2018b; Jiménez et al., 2018). This also indicates that the use of a "universal" rank is not efficient to properly reflect local vulnerabilities, and that this rank should reflect regional expected water level variations.

With respect to the tidal contribution, CVI's reflect very different vulnerability conditions because they consider the role played by this variable in a very different way. With independence of this, one of the observed features is that, unless the analysis is done at a very large spatial scale where tidal range can significantly vary, this component does not add significant information to discriminate the most vulnerable spots along the coast. This is the case of the study area where CVIs classified the entire coast as very high or very low vulnerable without any small-scale variation. In order to select how to account the role of tides in CVI, its contribution to the expected impact has to be properly considered. Although, as previously mentioned, different views can be adopted, it has to be considered that micro-tidal coastlines are very sensitive to SLR and their coastal ecosystems (Benassai et al., 2015), such as wetlands, are less resilient to water level changes (e.g. Cahoon and Guntenspergen, 2010).

Similarly to tides, the SLR component does not reflect any spatial variation. Again, this is a factor that will have relevance in large scale analysis where local conditions modify the expected sea level changes along the coast (e.g. Sallenger et al., 2012). Moreover, unless local data are derived from local observations, the use of sea level projections will also strongly condition a relatively homogeneous value with its contribution being given by the selected scenario, which will be a choice of the analyst.

As it has been highlighted, the use of the different methods may indicate a different vulnerability for a given coastal sector, in such a way that one grid cell can be evaluated from low to a very high vulnerability levels. Fig. 11 shows the spatial distribution of the variability in the overall relative vulnerability level indicated by the different methods along the study area computed for each 1 km cell. Obtained results indicate that the 5 percent of the 160 coastal cells present a difference in three vulnerability levels ranking from having a low to a very high vulnerability. Conversely, 25 percent of the grid cells are showing two vulnerability classes difference, which vary either from low to high or moderate to very high vulnerability. This reflects the importance of the selection of the method, although all tested method serve to assess coastal vulnerability they provide different information and this may lead to different decisions.

It is important to understand the effect of a calculation upon the resultant index and its distribution, while selecting a specific method for the integration of variables in calculation of a vulnerability index. Cogswell et al. (2018) stated that the CVI equation proposed by Gornitz (1991) is sensitive to the vulnerability class percentile divisions that are assigned due to the skewed index values. Therefore, the conversion of the overall vulnerability index scores into percentiles to divide them into various categories is usually subjective and subject to expert opinion (Fussel and Klein, 2006). Despite the knowledge of the experts on climate change and relevant risks, their opinion is not devoid of biases that may occur. Their priority shaped by their values and understanding of climate and social systems (Lowe and Lorenzoni, 2007) and their academic backgrounds (Hinkel et al., 2013) will affect the overall results in a vulnerability assessments.

Finally, as it can be deduced from this discussion, it is clear that although CVI's are useful tools for identifying vulnerable coastal areas, they need to be adequately used. Thus, a simple decision such as selecting a given method may have serious consequences from the management standpoint, since vulnerable hotspots can be identified in different locations. As an example, in the analyzed case whereas two methods classify the Maresme coastal stretch as mostly very high vulnerable, the other two ones significantly lower this classification. Moreover, it is also necessary to assess which is the partial contribution of each component to the overall vulnerability since this will also condition how expected differences will vary along the coast. Thus, in the analyzed case, in spite of the mentioned difference in Maresme, all methods classify the Llobregat coast as a very high vulnerable stretch. So, a priori is not possible to assume that a method is over or under predicting the overall vulnerability. Due to this, it is recommended that before to include the use of CVI as a tool to help in coastal risk management, to perform a sensitivity analysis and to select a ranking system properly reflecting local conditions.

6. Conclusions

Four different CVI computation approaches were applied to the 160 km long Barcelona (Spain) coastline, and results were compared and contrasted. As seen from the vulnerability categories of each variable and also the overall CVIs, the different approached reflect different vulnerability categories for the same grid cell. Among the CVI variables, the vulnerability categories of wave climate or wave height and shoreline change indicate minor differences for each CVI application. On the other hand, the most severe vulnerability class variations are

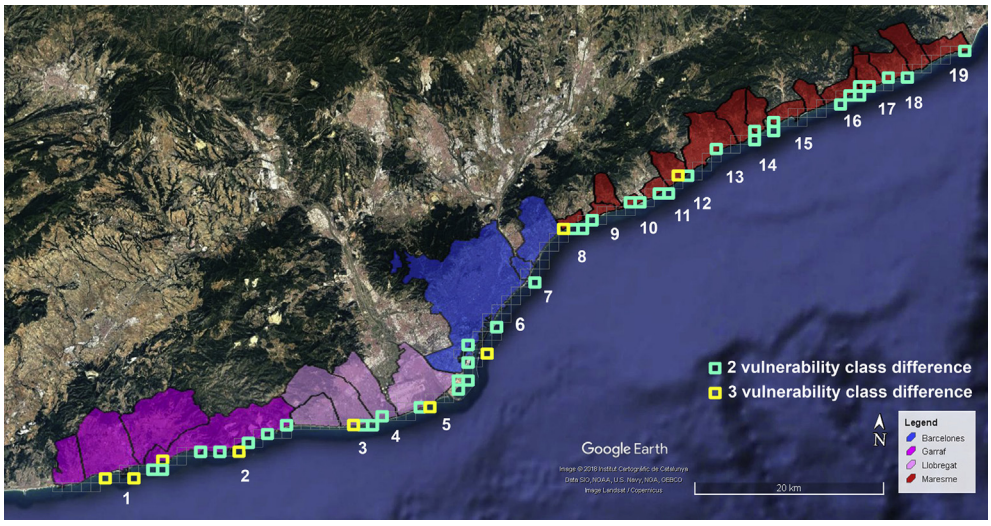

Fig. 11. Differences in vulnerability levels indicated by tested methods for each segment along the Barcelona coast.

seen in coastal slope and elevation, relative sea level rise, and tidal range variables.

Based on this analysis, Shaw et al. (1998) method appears to be the more realistic approach to assess vulnerability of the Barcelona coast. Taking into account the contribution of the maximum wave height and the tidal range to the overall CVI, the overall CVI scores and their distribution over cells, Shaw et al. (1998) approach indicates a higher number of areas with low and moderate vulnerability, compared to the other considered approaches.

Robust evaluation approaches, such as CVI applications, play an important role in facilitating future decision-making processes of coastal management strategies, especially in view adaptation to the increasing threats posed by climate change. However, it is important to reduce the need for subjective expert opinions in computing overall CVI scores.

This study shows that the ranking tables generated or adapted from databases of Pacific or Atlantic Coasts, may result in conflicting vulnerability results in other parts of the world. The large differences in vulnerability categories in each variable and overall CVIs point towards the need to develop site or region specific ranking categories. Also it shows that the methodology which is developed for and specific region with specific hydro-geomorphological condition is not always applicable to other regions.

Acknowledgements

The selected CVI ranking will be used in an ongoing project, “The Development of a Coastal Sustainability Index Scoring Tool (CoaSST),” as an input for the tool development process. This project has received funding from the European Union’s Seventh Framework Program for research, technological development and demonstration under grant agreement no 606838, with additional support from IHE Delft. The contribution of JAJ was done in the framework of the M-CostAdapt (CTM2017-83655-C2-1-R, MINECO/AEI/FEDER, UE) research project.

We would like to thank Prof. Harshinie Karunaratne from Swansea University, College of Engineering for comments on the manuscript, Üwe Sachelle Ntame Best and Dr. Seyedabdolhossein Mehvar from Water Sciences and Engineering Department of IHE Delft Institute for Water Education for the final editing and review of the manuscript.

References

Abuodha, P.A.O., Woodroffe, C.D., 2010. Assessing vulnerability to sea-level rise using a coastal sensitivity index: a case study from southeast Australia. J. Coast. Conserv. 14, 189–205.

Arns, A., Dangendorf, S., Jensen, J., Talke, S., Bender, J., Pattiaratchi, C., 2017. Sea-level rise induced amplification of coastal protection design heights. Sci. Rep. 7, 40171.

Arnell, N.W., Tompkins, E.L., Adger, W.N., 2005. Eliciting information from experts on the likelihood of rapid climate change. Risk Anal. 25 (6), 1419–1431. https://doi.org/10.1111/j.1539-6924.2005.00689.x.

Aucelli, P.P.C., Di Paola, G., Rizzo, A., Rosskopf, C.M., 2018. Present day and future scenarios of coastal erosion and flooding processes along the Italian Adriatic Coast: the case of Molise Region. Environ. Earth Sci. 77 (10). https://doi.org/10.1007/s12665-018-7535-y.

Aucelli, C.P.P., Di Paola, G., Incontri, P., Rizzo, A., Vilardo, G., Benassai, G., Buonocore, B., Pappone, G., 2017. Coastal inundation risk assessment due to subsidence and sea level rise in a Mediterranean alluvial plain (Volturno coastal plain e southern Italy). Estuarine. Estuar. Coast Shelf Sci 2016. https://doi.org/10.1016/j.ecss.2016.06.017.

Ballesteros, C., Jiménez, J.A., Valdemoro, H.I., Bosom, E., 2018. Erosion consequences on beach functions along the Maresme coast (NW Mediterranean, Spain). Nat. Hazards 90, 173–195.

Ballesteros, C., Jiménez, J.A., Viavattene, C., 2018b. A multi-component flood risk assessment in the Maresme coast (NW Mediterranean). Nat. Hazards 90, 265–292.

Benassai, G., Di Paola, G., Aucelli, P.P.C., 2015. Coastal risk assessment of a micro-tidal littoral plain in response to sea level rise. Ocean Coast Manag. 104, 22–35. https://doi.org/10.1016/j.ocecoaman.2014.11.015.

Bennett, W.G., Karunarathna, H., Mori, N., Reeve, D.E., 2016. Climate change impacts on future wave climate around the UK. J. Mar. Sci. Eng. 4, 78.

Boruff, B.J., Emrich, C., Cutter, S.L., 2005. Erosion hazard vulnerability of US coastal counties. J. Coast. Res. 21 (5), 932–942.

Bowman, D., Guillén, J., López, L., Pellegrino, V., 2009. Plan view Geometry and morphological characteristics of pocket beaches on the Catalan coast (Spain). Geomorphology 108, 191–199.

Brooks, N., Adger, W.N., 2005. Assessing and enhancing adaptive capacity. In: Lim, B., Spanger-Siegfried, E. (Eds.), Adaptation Policy Frameworks for Climate Change: Developing Strategies, Policies and Measures. United Nations Development Programme and Cambridge University Press, Cambridge, UK, pp. 165–181. http://www.preventionweb.net/files/7995_APF.pdf.

Bruun, P., 1962. Sea level rise as a cause of shore erosion. J. Waterw. Harb. Div. 88, 117–130.

Cahoon, D., Guntenspergen, G., 2010. Climate change, sea-level rise, and coastal wetlands. National Wetlands Newsletter 32, 8–12.

Carter, R.W.G., 1990. The Impact on Ireland of Changes in Mean Sea Level; Program of Expert Studies in Climate Change 2, vol. 128 Department of the Environment, Dublin.

CEDEX, 2014. Estrategia de actuacion en el Maresme. Ministerio de Fomento, Madrid.

CIIRC, 2010. Estat de la zona costanera a Catalunya. Resum Executiu. Generalitat de Catalunya, Barcelona.

Cogswell, A., B.J.W., Greenan, Greyson, P., 2018. Ocean Coast Manag. 160 (46), 51.

Cutter, S.L., Boruff, B., Shirley, W.L., 2003. Social vulnerability to environmental hazards. Soc. Sci. Q. 84 (2), 242–261. https://doi.org/10.1111/1540-6237.8402002.

Devoy, R., 2008. Coastal vulnerability and the implications of sea-level rise for Ireland. J. Coast. Res. 24 (2), 325–341.

Diez, P.G., Perillo, G.M.E., Piccolo, C.M., 2007. Vulnerability to sea-level rise on the coast of the buenos aires province. J. Coast. Res. 23, 119–126.

Doria, M. de F., Boyd, E., Tompkins, E.L., Adger, W.N., 2009. Using expert elicitation to define successful adaptation to climate change. Environ. Sci. Policy 12 (7), 810–819. https://doi.org/10.1016/j.envsci.2009.04.001.

Doukakis, E., 2005. Coastal vulnerability and sensitivity parameters. Eur. Water 11 (12), 3–7.

Duro, J., Inglada, J., Closa, J., Adam, N., Arnaud, A., 2004. High Resolution Differential Interferometry Using Time Series of ERS and Envisat SAR Data. Proc. Of FRINGE 2003. Workshop, ESA SP-550.

Emery, K.O., Aubrey, David G., 1991. Sea Levels, Land Levels, and Tide Gauges.

EEA, 2006. The Changing Faces of Europe's Coastal Areas. EEA Report No 6/2006. European Environment Agency, Copenhagen. www.eea.europa.eu/publications/eea_report_2006_6.

EEA, 2010. The European Environment. State of the Outlook 2010. Adapting to Climate Change. European Environment Agency, Copenhagen. www.eea.europa.eu/soer/europe/adapting-to-climate-change.

EEA, 2017. https://www.eea.europa.eu/data-and-maps/data/shoreline, Accessed date: 21 June 2017.

ESTAT, 2009. Nearly half of the population of EU countries with a sea border is located in coastal regions. Stat. Focus 47 2009.

Fussel, H.M., Klein, R.J.T., 2006. Climate change vulnerability assessments: an evolution of conceptual thinking. Clim. Change 75, 301–329.

Gibb, J., Sheffield, A., Foster, G., 1992. A Standardized Coastal Sensitivity Index Based on an Initial Framework for Physical Coastal Hazards Information. New Zealand Department of Conservation, pp. 101 Science and Research Series, No. 55.

Gornitz, V.M., Daniels, R.C., White, T.W., Birdwell, K.R., 1994. The development of a coastal risk assessment database: vulnerability to sea-level rise in the U.S. southeast. J. Coast. Res. 12, 327–338 Special Issue No.

Gornitz, V., 1991. Global coastal hazards from future sea level rise. Palaeogeogr. Palaeoclimatol. Palaeoecol. 89, 379–398.

Gornitz, V.M., 1990. Vulnerability of the East coast, U.S.A. to future sea level rise. J. Coast. Res. Special Issue 9, 201–237.

Gornitz, V., Kanciruk, P., 1989. Assessment of global coastal hazards from sea level rise. In: Coastal Zone 89, Proc. 6th Syrup. Coastal and Ocean Management/ASCE, pp. 1345–1359.

Gouldby, B., Samuels, P., 2005. Language of Risk, Project Definitions. FLOODsite Project Report, T32-04-01, EU GOCE-CT-2004-505420.

Gutierrez, B.T., Williams, S.J., Thieler, E.R., 2009. Basic approach for shoreline change projections. In: Titus, J.G., Anderson, K.E., Cahoon, D.R., Gesch, D.B., Gill, S.K., Gutierrez, B.T., Thieler, E.R., Williams, S.J. (Eds.), Coastal Sensitivity to Sea-Level Rise: A Focus on the MidAtlantic Region. A Report by the U.S. Climate Change Science Program and the Subcommittee on Global Change Research. U.S. Environmental Protection Agency, Washington DC, pp. 239–242. http://www.epa.gov/climatechange/effects/coastal/pdfs/SAP_41_SynthesisandAssessmentProduct.pdf.

Hemer, M.A., Wang, X.L., Weisse, R., Swail, V.R., 2012. Advancing wind-waves climate science: The COWCLIP project. Bull. Am. Meteorol. Soc. 93 (6), 791–796. https://doi.org/10.1175/BAMS-D-11-00184.1.

Hinkel, J., Bharwani, S., Bisaro, A., Carter, T., Cull, T., Davis, M., Klein, R., Lonsdale, K., Rosentrater, L., Vincent, K., 2013. PROVIA Guidance on Assessing Vulnerability, Impacts and Adaptation to Climate Change: Consultation Document. Global Programme of Research on Climate Change Vulnerability, Impacts and Adaptation (PROVIA). United Nations Environment Programme (UNEP), pp. 174.

ICGC, 2017. Institut Cartografic i Geologic de Catalunya. Generalitat de Catalunya. www.icc.cat, Accessed date: 28 July 2017.

IGME, 2017. Geológico y Minero de España. www.igme.es/cartografiadigital, Accessed date: 28 July 2017.

Intergovernmental Panel on Climate Change (IPCC), 2014. Climate change 2014: mitigation of climate change. In: Edenhofer, O., PichsMadruga, R., Sokona, Y., Farahani, E., Kadner, S., Seyboth, K., Adler, A., Baum, I., Brunner, S., Eickemeier, P., Kriemann, B., Savolainen, J., Schlömer, S., von Stechow, C., Zwickel, T., Minx, J.C. (Eds.), Contribution of Working Group III to the Fifth Assessment Report of the Intergovernmental Panel on Climate Change. Cambridge University Press, Cambridge, United Kingdom and New York, NY, USA.

IPCC, 2013. In: Stocker, T.F., Qin, D., Plattner, G.-K., Tignor, M., Allen, S.K., Boschung, J., Nauels, A., Xia, Y., Bex, V., Midgley, P.M. (Eds.), Climate Change 2013: the Physical

Science Basis. Contribution of Working Group I to the Fifth Assessment Report of the Intergovernmental Panel on Climate Change. Cambridge University Press, Cambridge, United Kingdom and New York, NY, USA, pp. 1535. https://doi.org/10.1017/CBO9781107415324.
IPCC, 2007. Climate change 2007: the physical science basis. In: Solomon, S., Qin, D., Manning, M., Chen, Z., Marquis, M., Averyt, K.B., Tignor, M., Miller, H.L. (Eds.), Contribution of Working Group I to the Fourth Assessment Report of the Intergovernmental Panel on Climate Change. Cambridge University Press, Cambridge, United Kingdom and New York, NY, USA.
IPCC, 2001. Climate Change 2001: the Scientific Basis. Contribution of Working Group I to the Third Assessment Report of the Intergovernmental Panel on Climate Change. Cambridge University Press, Cambridge.
Jiménez, J.A., Sancho, A., Bosom, E., Valdemoro, H.I., Guillen, J., 2012. Storm-induced damages along the Catalan coast (NW Mediterranean) during the period 1958-2008. Geomorphology 143–144, 24–33.
Jiménez, J.A., Valdemoro, H.I., Bosom, E., Sánchez-Arcilla, A., Nicholls, R.J., 2017. Impacts of sea-level rise-induced erosion on the Catalan coast. Reg. Environ. Change 17, 593–603.
Jiménez, J.A., Sanuy, M., Ballesteros, C., Valdemoro, H.I., 2018. The Tordera Delta, a hotspot to storm impacts in the coast northwards of Barcelona (NW Mediterranean). Coast. Eng. 134, 148–158.
Jiménez, J.A., Valdemoro, H.I., 2019. Shoreline evolution and management implications in beaches along the Catalan coast. In: Morales, J.A. (Ed.), The Spanish Coastal Systems. Dynamic Processes, Sediments and Management. Springer, pp. 745–764.
Leatherman, S.P., Clow, J.B., 1983. UMD shoreline mapping project. IEE Geosci. Remote Sens. Soc. Newsl. 22, 5–8.
Luijendijk, A., Hagenaars, G., Ranasinghe, R., Baart, F., Donchyts, G., Aarninkhof, S., 2018. The State of the World's Beaches. Sci. Rep. 8 Article number: 6641.
Lopez, R.,M., Ranasinghe, R., Jiménez, J.A., 2016. A rapid, low-cost approach to coastal vulnerability assessment at a national level. J. Coast. Res. 32 (4), 932–945.
Lowe, T.D., Lorenzoni, I., 2007. Danger is all around: Eliciting expert perceptions for managing climate change through a mental models approach. Glob. Environ. Chang. 17 (1), 131–146. https://doi.org/10.1016/j.gloenvcha.2006.05.001.
McLaughlin, S., Cooper, A., 2010. A Multi-scale coastal vulnerability index: A tool for coastal managers? Environ. Hazards 9 (3), 233–248. https://doi.org/10.3763/ehaz.2010.0052.
McLaughlin, S., McKenna, J., Cooper, A., 2002. Socio-economic data in coastal vulnerability indices: Constraints and opportunities. J. Coast. Res. 36, 487–497. https://doi.org/10.2112/1551-5036-36.sp1.487.
Mendoza, E.T., Jiménez, J.A., Mateo, J., 2011. A coastal storms intensity scale for the Catalan sea (NW Mediterranean) Nat. Hazards Earth Syst. Sci. 11, 2453–2462 2011.
Mendoza, E.T., Jiménez, J.A., 2009. Regional vulnerability analysis of Catalan beaches to storms. Marit. Eng. 162 (3). https://doi.org/10.1680/maen.2009.162.3.127.
Nageswara Rao, K., Subraelu, P., Venkateswara Rao, T., Hema Malini, B., Ratheesh, R., Bhattacharya, S., Rajawat, A.S., Ajai, 2008. Sea-level rise and coastal vulnerability: an assessment of Andhra Pradesh coast India through remote sensing and GIS. J. Coast. Conserv. 12, 195–207. https://doi.org/10.1007/s11852-009-0042-2.
Nicholls, R.J., Wong, P.P., Burkett, V., Codignotto, J., Hay, J., McLean, R., Ragoonaden, S., Woodroffe, C.D., 2007a. Coastal systems and lowlying areas. In: Parry, M.L., Canziani, O.F., Palutikof, J.P., van der Linden, P., Hanson, C.E. (Eds.), Climate Change 2007: Impacts, Adaptation and Vulnerability. Contribution of Working Group II to the Fourth Assessment Report of the Intergovermental Panel on Climate Change. Cambridge University Press, Cambridge, pp. 315–357.
Nicholls, R.J., Hanson, S., Herweijer, N., Patmore, N., Hallegatte, S., Corfee-Morlot, J., Chateau, J., Muir-Wood, R., 2008. Ranking port cities with high exposure and vulnerability to climate extremes: Exposure estimates. OECD Environ. Work. Pap. 1, 63. OECD Publishing, Paris. https://doi.org/10.1787/19970900.
Ojeda, E., Guillén, J., 2008. Shoreline dynamics and beach rotation of artificial embayed beaches. Mar. Geol. 253 (1–2), 51–62.
Ozyurt, G., Ergin, A., 2010. Improving Coastal Vulnerability Assessments to Sea-Level Rise: A New Indicator-Based Methodology for Decision Makers. J. Coast. Res. 26 (2), 265–273.
Pendleton, E.A., Thieler, E.,R., Williams, S.J., Beavers, R.S., 2004. Coastal Vulnerability Assessment of Padre Island National Seashore (PAIS) to Sea-Level Rise. USGS report No 2004–1090 Available from: http://pubs.usgs.gov/of/2004/1090/a.
Puertos del Estado, 2017. http://www.puertos.es/en-us/oceanografia/Pages/portus.aspx, Accessed date: 30 September 2017.
Python Software Foundation Python Language Reference, version 3.6.5. Available at: http://www.python.org.
Ranasinghe, R., 2016. Assessing Climate change impacts on Coasts: A Review. Earth Sci. Rev. 160, 320–332.
Ranasinghe, R., Duong, T., Uhlenbrook, S., Roelvink, D., Stive, M., 2013. Climate Change impact assessment for inlet-interrupted coastlines. Nat. Clim. Change 3, 83–87.
Ranasinghe, R., Callaghan, D., Stive, M., 2012. Estimating coastal recession due to sea level rise: Beyond the Bruun Rule. Clim. Change 110 (3–4), 561–574.
Ranasinghe, R., Stive, M.J.F., 2009. Rising seas and retreating coastlines. Clim. Change 97, 465–468. https://doi.org/10.1007/s10584-009-9593-3.
Rosen, P.S., 1977. Increasing shoreline erosion rates with decreasing tidal range in the Virginia Chesapeake Bay. Chesap. Sci. 18 (4), 383–386.
Sallenger Jr., A.H., Doran, K.S., Howd, P.A., 2012. Hotspot of accelerated sea-level rise on the Atlantic coast of North America. Nature Climate Change 2, 884–888.
Shaw, J., Taylor, R.B., Forbes, D.L., Ruz, M.-H., Solomon, S., 1998. Sensitivity of the coasts of Canada to sea-level rise. Bull. Geol. Surv. Can. 505, 1–79.
Slott, J.M., Murray, A.B., Ashton, A.D., Crowley, T.J., 2006. Coastline responses to changing storm patterns. Geophys. Res. Lett. 33.
Smith, J.B., Schneider, S.H., Oppenheimer, M., Yohe, G.W., Hare, W., et al., 2009. Assessing dangerous climate change through an update of the Intergovernmental Panel on Climate Change (IPCC) 'reasons for concern'. Proc. Natl. Acad. Sci. Unit. States Am. 106 (11), 4133–4137. https://doi.org/10.1073/pnas.0812355106.
Snoussi, M., Ouchani, T., Niazi, S., 2008. Vulnerability assessment of the impact of sea-level rise and flooding on the Moroccan coast: The case of the Mediterranean eastern zone. Estuarine. Estuar. Coast Shelf Sci. 77, 206–213.
Sterl, A., van den Brink, H., de Vries, H., Harsma, R., van Meijgaard, E., 2009. An ensemble study of extreme storm surge related water levels in the North Sea in a changing climate. Ocean Sci. 5, 369–378.
Sterr, H., 2008. Assessment of vulnerability and adaptation to sea-level rise for the coastal zone of Germany. J. Coast. Res. 24 (2), 380–393.
Svetlana, J., Moore, J.C., Grinsted, A., Woodworth, P.L., 2008. Recent global sea level acceleration started over 200 years ago? Geophys. Res. Lett. 35 (8).
Thieler, E.R., Hammar-Klose, E.S., 2000. National Assessment of Coastal Vulnerability to Future Sea-Level Rise: Preliminary Results for the U.S. Pacific Coast: U.S. Geological Survey, Open-File Report 00-178.
Thieler, E.R., Hammar-Klose, E.S., 1999. National Assessment of Coastal Vulnerability to Sea-Level Rise, U.S. Atlantic Coast. US Geological Survey, Open-File Report. pp. 99–593.
Thieler, E.R., Himmelstoss, E.A., Zichichi, J.L., Ergul, Ayhan., 2009. Digital Shoreline Analysis System (DSAS) Version 4.0 — an ArcGIS Extension for Calculating Shoreline Change. Report 2008-1278. U.S. Geological Survey Open-File.
Vermeer, M., Rahmstorf, S., 2009. Global sea level linked to global temperature. Proc. Natl. Acad. Sci. Unit. States Am. 106, 21527–21532.
Woodruff, J.D., Irish, J.L., Camargo, S.J., 2013. Coastal flooding by tropical cyclones and sea-level rise. Nature 504, 44–52. https://doi.org/10.1038/nature12855.